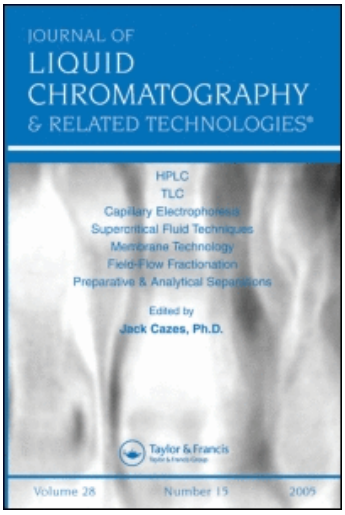

Journal of Liquid Chromatography & Related Technologies
Publication details, including instructions for authors and subscription information:
http://www.informaworld.com/smpp/title~content=t713597273

Speculation on the Mechanism of Unilateral Hydrodynamic Distribution of Two Immiscible Solvent Phases in the Rotating Coil

Yoichiro Ito[a]
[a] NIH-NHLBI, Bethesda, Maryland

To cite this Article Ito, Yoichiro(1992) 'Speculation on the Mechanism of Unilateral Hydrodynamic Distribution of Two Immiscible Solvent Phases in the Rotating Coil', Journal of Liquid Chromatography & Related Technologies, 15: 15, 2639 — 2675
To link to this Article: DOI: 10.1080/10826079208016340
URL: http://dx.doi.org/10.1080/10826079208016340

JOURNAL OF LIQUID CHROMATOGRAPHY, 15(15&16), 2639-2675 (1992)

SPECULATION ON THE MECHANISM OF UNILATERAL HYDRODYNAMIC DISTRIBUTION OF TWO IMMISCIBLE SOLVENT PHASES IN THE ROTATING COIL

YOICHIRO ITO
NIH-NHLBI
Bethesda, Maryland 20892

ABSTRACT

The proposed hypothesis is based on the interplay between two force components acting on the fluid in the rotating coil. The tangential force component generates the Archimedean screw effect to move two solvent phases toward the head of the coil whereas the radial force component acts against the Archimedean force to establish a hydrostatic distribution of the two phases throughout the coil. The unilateral hydrodynamic distribution of the two phases is governed by the degree of asymmetry in the radial force field on the coil in both simple rotation and synchronous planetary motion. The present hypothesis successfully explains all the observed hydrodynamic phenomena reported in the past.

INTRODUCTION

Countercurrent chromatography (CCC) utilizes an intriguing hydrodynamic behavior of two immiscible solvent phases through a tubular column space free of solid support matrix [1]. Retention of the stationary

phase and solute partitioning take place under the suitable combination of the column configuration and applied force field. The most versatile form of CCC called the hydrodynamic equilibrium system uses a rotating coil in an acceleration field, i.e., either in the unit gravity or in the centrifugal force filed. Two immiscible solvents confined in such a coil distribute themselves along the length of the coil to form various patterns of hydrodynamic equilibrium.

Since 1970s, experimental observations performed in the course of developing the CCC technology have disclosed a number of strange hydrodynamic phenomena taking place in the rotating coil. In general two immiscible solvent phases in a rotating coil form two contrasting distribution patterns: one is called the basic hydrodynamic equilibrium and the other unilateral hydrodynamic equilibrium [2]. In the basic hydrodynamic equilibrium the two solvent phases are evenly distributed from one end of the coil called the head and any excess of either phase is accumulated at the other end called the tail. Here, the head-tail relationship of the rotating coil is defined by the direction of the Archimedean screw force which drives all objects toward the head of the coil. In the unilateral hydrodynamic equilibrium, the two solvent phases are unilaterally distributed along the length of the coil, one phase (head

phase) entirely occupying the head side and the other phase (tail phase), the tail side of the coil. In this unilateral distribution, the head phase can be the lighter or the heavier phase and also can be the aqueous or the nonaqueous phase depending upon the physical properties of the solvent system and the applied experimental condition. These hydrodynamic distribution studies have been carried out mainly on three different rotary motions of the coil, i.e., simple rotation in the unit gravitational field and two different modes of the synchronous planetary motion each provided by a particular type of the coil planet centrifuge. In the following, the typical results of those studies are summarized to review complex hydrodynamic behavior of the two solvent phases in the rotating coil.

HYDRODYNAMIC DISTRIBUTION OF TWO SOLVENT PHASE IN THE ROTATING COIL

Rotating Coil assembly [3]

Fig. 1 illustrates distribution of two immiscible solvent phases in rotating coil in the unit gravitational field. Experiments were performed with a 5.5mm ID FEP (fluorinated ethylene propylene) tubing coiled around the cylindrical holder which was held horizontally to rotate around its own axis. A two-phase solvent system composed of chloroform/acetic acid/0.1M hydrochloric acid (2:2:1)

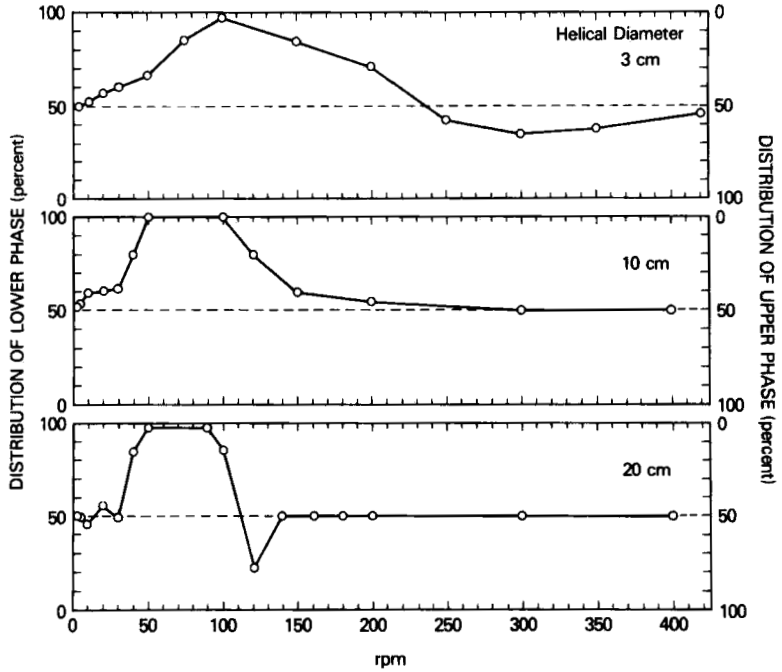

FIGURE 1. Phase distribution diagram for coaxially rotating coils with three different helical diameters. Simple coil rotation in the unit gravity forms a complex distribution curve which may be divided into four stages.

was equilibrated in a separatory funnel with a small amount of Sudan III to color the nonaqueous phase for facilitating observation of phase distribution through the transparent tube wall. The coil was first filled with equal volumes of the lighter and heavier phase, sealed at both ends, and then rotated at a given rate. After the two solvent phases reached the hydrodynamic equilibrium state, the volume of each phase occupying on the head

side of the coil was noted, the process being repeated by changing the rate of rotation. The volume percentage of each phase occupying the head side of the coil was calculated and plotted against the applied rpm to make a phase distribution diagram. The above studies were made on the coils with three different helical diameters, i.e., 3cm, 10cm and 20cm as indicated in Fig. 1.

All three diagrams revealed a common feature of the phase distribution pattern: At the slow rotational speed of 0-30 rpm, the two solvent phases establish the basic hydrodynamic equilibrium to distribute fairly evenly in the coil (Stage I). As the rotational speed is increased, the heavier nonaqueous phase starts to occupy more space on the head side of the coil and, at the critical rotational speed between 60 and 100 rpm, the two phases establish unilateral hydrodynamic equilibrium where the heavier phase entirely occupies the head side of the coil (Stage II). After this critical range of rpm, the amount of the heavier phase on the head side decreases rapidly crossing below the 50% line (Stage III). Further increase of the rotational speed again yields and even distribution of the two phases in the coil (Stage IV). As the helical diameter is increased, all these stages are shifted toward the lower rpm range apparently due to the enhanced centrifugal force field.

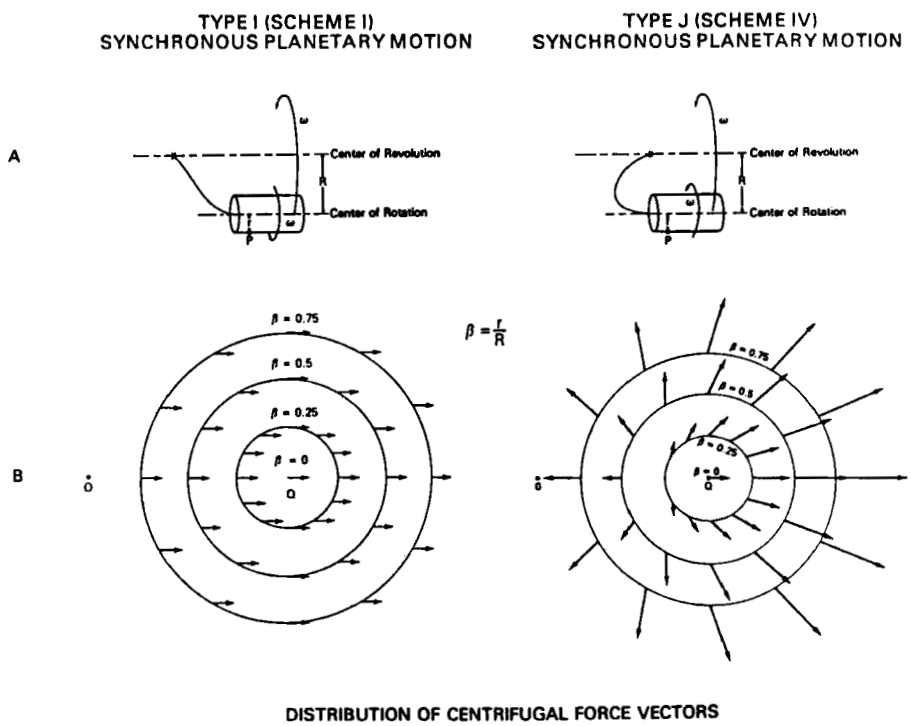

FIGURE 2. Two types of synchronous planetary motion and their centrifugal force fields.

Synchronous Coil Planet Centrifuge [4,5]

Fig. 2A shows two typical synchronous planetary motions of a cylindrical coil holder equipped with a bundle of flow tubes. In Type I planetary motion (left), the holder revolves around the central axis of the centrifuge and simultaneously counterrotates about its own axis at the same angular velocity. In Type J planetary motion (right), the holder undergoes a similar

planetary motion except that rotation and revolution of the holder are both in the same direction. As described earlier [1,4], these synchronous planetary motions permit the flow tubes to remain entirely twist-free and, therefore, continuous elution through the rotating coiled column becomes possible without the use of rotary seals.

Distribution of the centrifugal force vectors on the rotating holder is illustrated in Fig. 2B where O indicates the center of revolution and Q, the center of rotation. The location of the point on the holder is expressed by a single parameter, ß=r/R, where r is the rotation radius (distance from the axis of the holder to point P) and R, the revolution radius (distance between the axis of the holder and the central axis of the apparatus). In Type I synchronous planetary motion, every location on the holder is subjected to an identical force field regardless of the ß values. As the holder revolves around the central axis of the centrifuge, the field rotates at the same angular velocity in the same direction. On the other hand, Type J synchronous planetary motion produces a highly complex heterogeneous force filed which varies in both magnitude and direction according to the location of the point on the holder. However, when the ß value exceeds 0.25, the centrifugal force vectors are always directed outwardly from the holder.

The phase distribution studies performed with various two-phase solvent systems in a coiled column have demonstrated a contrasting difference between these two synchronous planetary motions. In the coiled column with internal diameters of 1.2 mm or greater (where the effects of solvent-wall interaction to form a plug flow become insignificant), Type I synchronous planetary motion produces a basic hydrodynamic equilibrium under a broad range of revolution speed [5,6]. On the other hand, Type J synchronous planetary motion produces a unilateral hydrodynamic equilibrium where the head phase is determined by various physical properties of the solvent system as summarized in Table 1 [7,8]. Hydrophobic binary solvent systems with high interfacial tension and low viscosity such as hexane/water, ethyl acetate/water and chloroform/water, always distribute the lighter phase on the head side and the heavier phase on the tail side. Hydrophilic solvent systems characterized by low interfacial tension and high viscosity including n-butanol/acetic acid/water (4:1:5) and sec.-butanol/water show the opposite hydrodynamic behavior and always distribute the heavier phase on the head side and the lighter phase on the tail side. In the rest of the solvent systems with intermediate hydrophobicity between the above two extremes, the head phase is determined by the ß values of the coiled column. With large ß values

TABLE 1
Comparison Between Three Solvent Groups in Their Settling Times and Unilateral Hydrodynamic Distribution in the Rotation coil

Solvent Group	Solvent System* (Volume Ratio)	Settling Time (sec)	Unilateral Hydrodynamic Distribution
Hydrophobic	Hexane/H_2O	<1	upper phase
	CH_3Cl/H_2O	2.5	
	EtOAc/H_2O	15.5	
Intermediate	EtOAc/AcOH/H_2O (4:1:4)	15.0	upper phase with large ß lower phase with small ß
	n-BuOH/H_2O	18.0	
	CH_3Cl/AcOH/H_2O (2:2:1)	29.0	
Hydrophilic	n-BuOH/AcOH/H_2O (4:1:5)	38.5	lower phase
	sec.-BuOH/H_2O	57.0	

* EtOAc: ethyl acetate; AcOH: acetic acid; BuOH: butanol.

the lighter phase becomes the head phase as in the hydrophobic solvent systems while with small ß values the heavier phase becomes the head phase as in the hydrophilic solvent systems. Each solvent group exhibits a different range of settling times which are required for the two-phase mixture to separate into two layers in the unit gravity (Table 1) [8]. The hydrophobic solvent systems show the shortest settling times of several seconds; the hydrophilic solvent systems, the longest settling times of over 30 seconds; and the intermediate solvent systems, moderate settling times between those of the above extremes.

The hydrodynamic motion of the two solvent phases has been directly observed under stroboscopic illumination [9]. A spiral column prepared from 1.6 mm ID PTFE tubing was coaxially mounted on the holder of a Type-J synchronous coil planet centrifuge. A two-phase solvent system composed of chloroform/acetic acid/water (2:2:1) was colored red and yellow with dyes. The spiral column was filled with the stationary phase and then eluted with the mobile phase at 240 ml/h in a proper mode while the apparatus was spun at 800 rpm. The stroboscopic observation revealed that the column was divided into two distinct zones, the mixing zone and the settling zone as shown in Fig. 3. The mixing zone locally extends about one fourth of the area near the

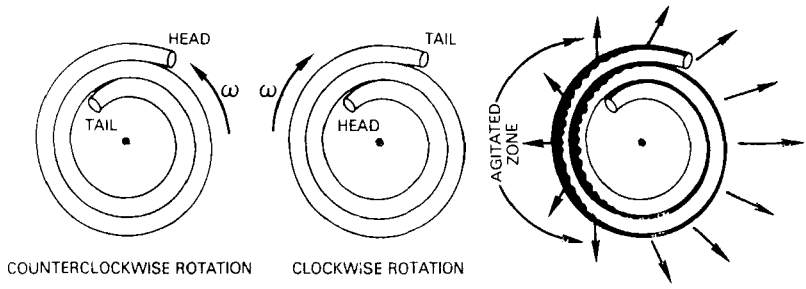

FIGURE 3. Mixing and settling zones in the rotating spiral column.

center of the centrifuge and shows evidence of vigorous agitation of the two layers. In the rest of the area, the two phases are clearly separated into two layers, heavier phase occupying the outer portion and the lighter phase, the inner portion of each spiral segment.

HYPOTHESIS ON THE MECHANISM OF HYDRODYNAMIC DISTRIBUTION

The diverse hydrodynamic phenomena described above serve as useful materials for developing a hypothesis on the mechanism of hydrodynamic distribution of two solvent phases in the rotating coil. Any hypothesis proposed for the above subject must be challenged to answer all of the following questions:

1. Why does the hydrodynamic phase distribution in the rotating coil follow four different stages?
2. Why do the two types of synchronous planetary

motion produce the contrasting hydrodynamic distribution?

3. In the unilateral hydrodynamic equilibrium what determines the phase that will preferentially occupy the head of the coil?
4. How are the mixing and settling zones formed in the coil undergoing Type J planetary motion?

The hypothesis introduced below in this paper will give satisfactory answers to all of the above problems and serve as a stepping stone for further establishing a theory on this complex hydrodynamic phenomena in the rotating coil.

The present hypothesis tries to explain the whole complexity of the above hydrodynamic phenomena on the basis of the interplay between two force components: one component (F_t) acts tangentially along the coil to produce an Archimedean screw effect to move two solvent phases toward the head while the other component (F_r) acts radially across the diameter of the coiled tube to interfere with relative motion of the two solvent phases against the Archimedean screw force causing a hydrostatic distribution of the two phases around each helical turn.

Rotating Coil in the Unit Gravity

In the phase distribution diagram obtained from the rotating coil in the unit gravity (Fig. 1), the effects

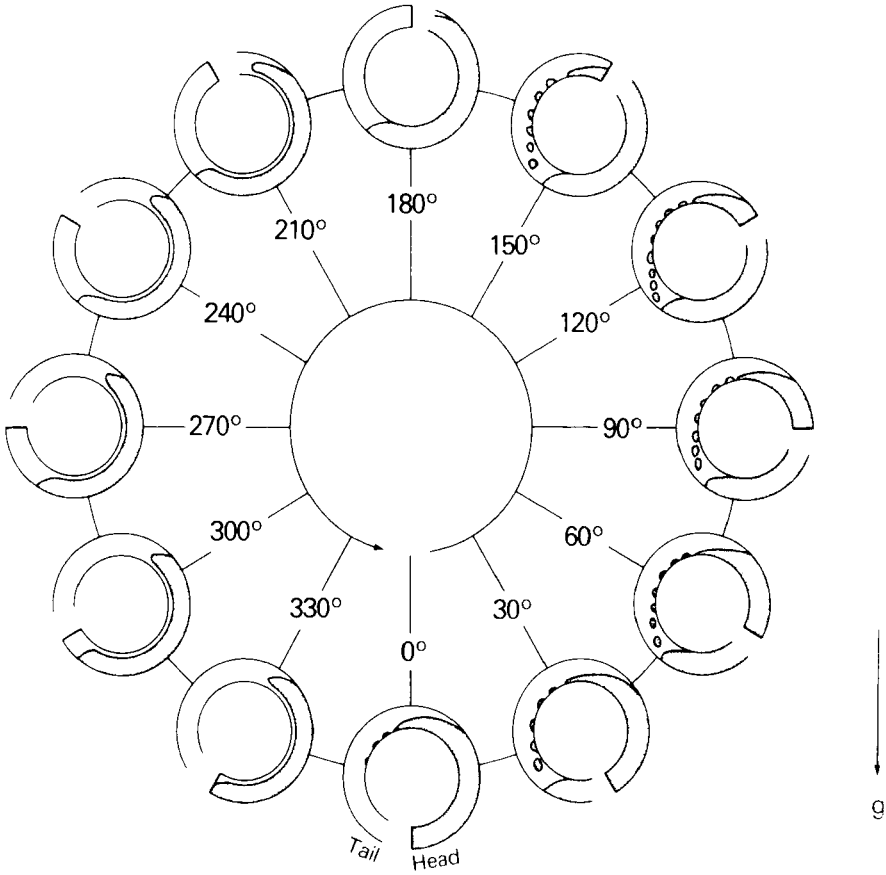

FIGURE 4. Motion of two immiscible zones in the rotating coil under the basic hydrodynamic equilibrium state. Successive positions of the slowly rotating coil show back and forth movement of the two solvent phases during one complete turn. The lighter phase initiates advancing toward the head at the top of the coil (the upper key node) and the heavier phase initiates advancing toward the head at the bottom of the coil (the lower key node).

of these two force components are locally well isolated from each other. At a slow rotational speed where action of the centrifugal force is negligible, the two solvent phases are evenly distributed by the Archimedean screw force (F_t) to establish the basic hydrodynamic equilibrium at the head side of the coil (Stage I). The effects of the radially acting force component (F_r) is observed at a high revolution speed where the two solvent phases are hydrostatically distributed throughout the coil, the heavier phase occupying the outer portion and the lighter phase occupying the inner portion of each helical turn (Stage IV). At the intermediate speed range between the above extremes, the two force components display a complex interaction to form a strange-looking undulating curve in the phase distribution diagram. In order to understand the mechanism underlying this hydrodynamic process, one must closely observe the motion of the two solvent phases in the rotating coil.

Fig. 4 illustrates the hydrodynamic motion of two immiscible solvent phases at the head of a slowly rotating coil observed under the basic hydrodynamic equilibrium condition. As clearly shown in successive positions of the rotating coil, during rotation between 0 and 180 degrees the heavier phase percolates through the lighter phase segment on the left half of the coil resulting in advancement of the lighter phase toward the

head end. Similarly, during coil rotation between 180 and 0 degrees the lighter phase streams up through the heavier phase on the right half of the coil resulting in advancement of the heavier phase toward the head. Under the basic hydrodynamic equilibrium state, the above alternate back and force fluxing of the two solvent phases repeats in each rotation in every helical turn from the head to the tail throughout the portion of the coil containing the two solvent phases.

In this repetitive hydrodynamic process, flux of each phase always begins at the top or the bottom of the rotating coil: The lighter phase starts advancing toward the head end at the top of the coil (the upper key node) and the heavier phase starts advancing toward the head end at the bottom of the coil (the lower key node). This fact bears an extremely important implication that the hydrodynamic condition at the top and the bottom of the coil would impose critical effects on the action of the Archimedean screw force to distribute the two solvent phases unevenly in the rotating coil. For example, if any unfavorable hydrodynamic condition such as emulsification of the solvents is locally present at the top of the coil, it would hamper the advancement of the lighter phase toward the head resulting in a dominant or even unilateral hydrodynamic distribution of the heavier phase on the head side of the coil. Consequently, any

asymmetrical hydrodynamic condition between the top and the bottom of the rotating coil could cause the unilateral hydrodynamic equilibrium with the head phase, either the lighter or the heavier phase, whichever provided more favorable hydrodynamic conditions.

Using the above concept, one can easily rationalize the shape of the phase distribution curve illustrated in Fig. 1. At slow rotation, the top and bottom of the coil are similarly subjected to the unit gravitational field and the two solvent phases establish the basic hydrodynamic equilibrium, each occupying near 50% of the space in the head side of the coil. As the rotational speed increases, radially acting centrifugal force (F_r) begins to exert a significant influence on the action of the Archimedean screw force (F_t). While the radial centrifugal force acts symmetrically around every portion of the coil, the unit gravitational field acts vertically also at every portion of the coil. Consequently, the sum of these two forces forms a heterogeneous force field that acts asymmetrically between the upper and the lower portions of the coil. At the top of the coil the centrifugal force acts in the opposite direction to the gravity and reduces the strength of the force field, whereas at the bottom of the coil both the centrifugal force and the gravity act in the same direction and therefore increase the strength of the force field. As

described earlier, this asymmetric force field creates unbalanced hydrodynamic motion between the two solvent phases. Since the applied two-phase solvent system contains a large amount of acetic acid to moderate the interfacial tension, the increased force field at the bottom of the coil may initially provide a more favorable hydrodynamic condition for the heavier phase to advance toward the head by coalescing the droplets, while the decreased force filed at the top of the coil provide less favorable hydrodynamic condition for the lighter phase to advance toward the head by accelerating the droplet formation. As a result the heavier phase gradually occupies more space at the head end and at the critical rotational range between 80 and 120 rpm the two solvent phases establish the unilateral hydrodynamic equilibrium with the heavier phase on the head side of the coil (Stage II).

When the rotational speed of the coil is further increased above this critical range, the force field at the bottom of the coil gains strength and begins to hamper the relative movement of the two solvent phases while the force field at the top of the coil passes the zero point and thereafter starts to increase its strength, thus facilitating advancement of the lighter phase toward the head. This results in a reversed hydrodynamic distribution of the two solvent phases at

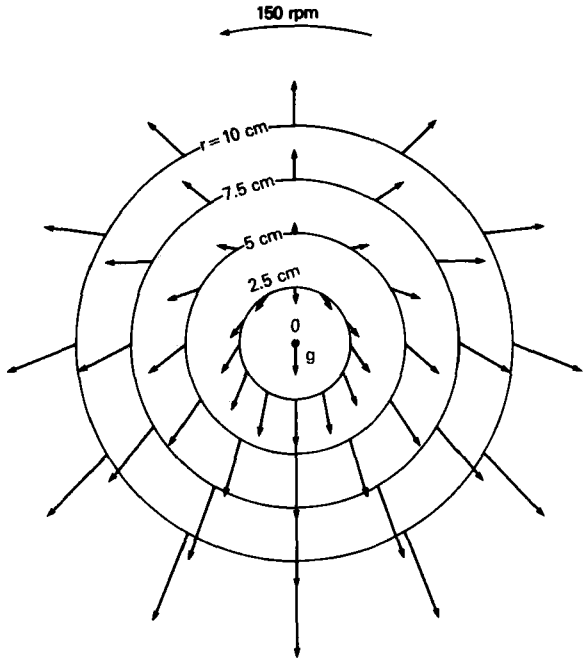

FIGURE 5. Force distribution diagram of a rotating disc in the unit gravity at 150 rpm.

the head hence the phase distribution curve falls crossing down the 50% line in Fig. 1 (Stage III). However, the force field at the top and the bottom of the coil soon reaches the critical magnitude to hamper the action of the Archimedean screw force and finally the two solvent phases are hydrostatically distributed evenly throughout the coil (Stage IV). The use of a large helical diameter coil enhances the centrifugal force field as a given rpm to accelerate the whole hydrodynamic

process resulting in the shift of the phase distribution curve toward the left.

The combined force field of the centrifugal and gravitational components acting on the rotating coil at 150 rpm is analyzed and illustrated in Fig. 5 using a similar force distribution format shown in Fig. 2B. Several concentric circles indicate coils with different helical diameters (2r). The overall force distribution pattern bears a remarkable resemblance to that obtained from Type J synchronous planetary motion (Fig. 2B, right), while the force distribution produced from the rotating coil at slow rpm is almost identical to that obtained from Type I synchronous planetary motion (Fig. 2B, left). This fact strongly suggests that the present hypothesis may well be extended to the hydrodynamics for the two solvent phases in the coil undergoing the synchronous planetary motion.

Synchronous Planetary Motion

Type I synchronous planetary motion produces a homogeneous distribution of the force vectors through all locations on the holder as illustrated in Fig. 2B, left. In this force distribution diagram, there are two key points as in the rotating coil in the unit gravity described earlier. The point nearest to the center of revolution (the proximal key node) corresponds to the

upper key node of the rotating coil in the unit gravity where the lighter phase initiates advancement toward the head. The point farthest from the center of revolution (the distal key node) corresponds to the lower key node of the rotating coil in the unit gravity where the heavier phase initiates advancement toward the head. As clearly shown in Fig. 2B (left), these two key nodes are subjected to the identical force field and, therefore, the two solvent phases establish the basic hydrodynamic equilibrium regardless of their physical properties as in a slowly rotating coil in the unit gravity but under a high revolution speed of the coil.

Type J synchronous planetary motion (Fig. 2, right) generates a heterogeneous distribution of the centrifugal force vectors similar to that obtained from a rotating coil in the unit gravity at a moderate rate (Fig. 5). As in Type I synchronous planetary motion, each turn of the coil (coaxially mounted on the holder) bears a pair of key nodes where the Archimedean screw force reverses its direction with respect to the coil: The proximal key node triggers the movement of the lighter phase toward the head and the distal key node triggers the movement of the heavier phase toward the head. As clearly illustrated in the force distribution diagram (Fig. 2B, right), the forces acting at these two key nodes show different magnitude: Magnitude of the force acting at the distal

key node on the coil always exceeds that acting at the proximal key node on the coil while both forces gain their strength as the helical diameter of the coil increases. This asymmetry of the force field will provide basis for understanding the mechanism of the unilateral hydrodynamic distribution produced by various two-phase solvent systems.

Hydrodynamic solvent systems including hexane/water, ethyl acetate/water, and chloroform/water, are characterized by high interfacial tension and low viscosity of the nonaqueous phase. Because of these unique physical properties, these binary solvent systems exhibit short settling times in the rotating coil and, therefore, presence of the radial force component (F_r) would always interfere with the relative movement of the two solvent phases along the coil. Thus, in these solvent systems the lighter phase always receive more favorable hydrodynamic condition at the proximal portion of the coil to advance toward the head regardless of the helical diameter of the coil.

On the other hand, hydrophilic solvent systems such as n-butanol/acetic acid/water (4:1:5) and sec.-butanol/water possess contrasting physical properties to the above hydrophobic solvent systems. Because of their low interfacial tension, high viscosity, and relatively small density difference between the two phases, these

solvent systems exhibit high tendency of emulsification and, therefore, would require extremely long settling time in the rotating coil. Under these circumstances, radial force component (F_r) would always provide rather favorable hydrodynamic conditions for relative movement of the two solvent phases in the rotating coil. Thus, in these hydrophilic solvent systems the heavier phase always receives a more favorable hydrodynamic condition to become the head phase.

The rest of the two-phase solvent systems such as chloroform/acetic acid/water (2:2:1) and ethyl acetate/acetic acid/water (4:1:4) possess physical properties intermediate between the above two extremes. Because of the moderate interfacial tension between the two phases, these solvent systems form small droplets under vigorous agitation and require the settling times significantly longer that those for the hydrophobic solvent systems. Under these conditions the radial force component (F_r) exerts two mutually opposing effects on the relative motion of the two solvent phases in the rotating coil. The radially acting force (F_r) can initially facilitate the action of the Archimedean screw force (F_t) by accelerating coalescence of droplets into two layers but it will eventually interfere with the relative movement of the two solvent phases through the coil.

In a small helical diameter of the coil (small ß), where the magnitude of the radial force component (F_r) is relatively small, the heavier phase in the distal portion of the coil receives the favorable hydrodynamic condition to initiate advancement toward the head while the advancement of the lighter phase is retarded by formation of numerous droplets at the proximal portion of the coil. Consequently, the heavier phase becomes the head phase as observed in the hydrophilic solvent systems. In a large helical diameter coil (large ß), where the magnitude of the radial force component (F_r) becomes increased, advancement of the heavier phase is hampered by a strong radial force component (F_r) acting at the peripheral portion of the coil, thence the lighter phase receives more favorable hydrodynamic condition at the proximal portion of the coil to initiate advancement toward the head. Consequently, the lighter phase becomes the head phase as in the hydrophobic solvent systems. As described above, the present hypothesis can provide reasonable explanation on the mechanism of hydrodynamic distribution of various two-phase solvent systems in the rotating coil.

Recent findings of the stroboscopic observation on two-phase flow through the running spiral column by Dr. W.D. Conway et al. [9,10] may also be explained on the basis of the present hypothesis. When the lower phase is

eluted through the stationary lighter phase from the internal head toward the external tail of the spiral column (Fig. 3, middle), a large volume of the stationary phase is retained in the column while the spiral column is divided into two distinct zones, the mixing zone in about one fourth of the area near the center of the centrifuge and the settling zone showing a linear interface between the two phases in the rest of the area (Fig. 3, right). The center of the mixing and settling zones coincides with the proximal and the distal key nodes, respectively. At the distal portion of the rotating column, the strong radial force component (F_r) acting across the diameter of the tube largely interferes with the relative motion of the two solvent layers and both phases move at the almost equal rates toward the tail (outlet) of the spiral column. At this distal portion of the coil, both the strong radial force field and the reduced relative flow of the two phases establish a clear and stable interface between the two solvent phases as observed under the stroboscopic illumination.

In the proximal portion of the spiral column, where the strength of the radial force component (F_r) is minimum, the effect of the Archimedean screw force (F_t) becomes visualized as vigorous agitation at the interface caused by the relative movement of the two solvent layers. At the ascending loop on the head side (Fig. 3,

right, lower portion of the spiral segments) the relative motion of the two solvent phases consists of downward motion of the heavier phase toward the head and upward motion of the lighter phase toward the tail. At the proximal portion of the ascending loop where the Archimedean screw force (F_t) becomes reduced, the relative motion of the two phases decreases and at the proximal key node the two phases move together toward the tail at the pumping rate where the relative movements of the two solvent layers is mainly effected their difference in viscosity. At the descending loop on the tail side (Fig. 3, right, upper portion of the spiral segments) where the action of the Archimedean screw force (F_t) is reversed, the two solvent phases resume the relative movement in the opposite direction in such a way that the heavier phase moves downward toward the tail and the lighter phase upward toward the head. Under the favorable hydrodynamic condition around the proximal node, the relative motion between the two layers smoothly gains the acceleration in the descending loop until the motion is interfered with the increasing strength of the radial force component (F_r). Thus, retention of the stationary lighter phase is ensured by a rapid back flux of the lighter phase through the descending spiral loops that compensates forward the movement of the lighter phase in the rest of the spiral column. By analogy with

the rotating coil in the unit gravity (Fig. 4), the reversal of the relative motion of the two phases between the ascending and descending loops alternately repeats at the rate of revolution or over 13 times per second (at 800rpm). Consequently, the repetitive deceleration and acceleration in the relative motion between the two solvent layers at such a high frequency creates vigorous agitation at their interface in the proximal portion of the spiral loop where the stabilizing action of the radial force component (F_r) is also minimized.

ANALYSIS OF RADIAL AND TANGENTIAL FORCE COMPONENTS ON THE ROTATING COIL

In the foregoing, various hydrodynamic phenomena observed in the rotating coils have been rationalized on the basis of interplay between the tangential and radial force components where an asymmetry of the force field on the rotating coil creates various patterns of distribution of the two solvent phases. Below, simple mathematical analyses of these two force components have been carried out on the three forms of rotary systems, i.e., two types of synchronous planetary motion and simple rotation in the unit gravitational field.

Fig. 6 summarizes the results of the above analysis where the top diagrams show motion of the coil holder in the three rotary systems together with the coordinate

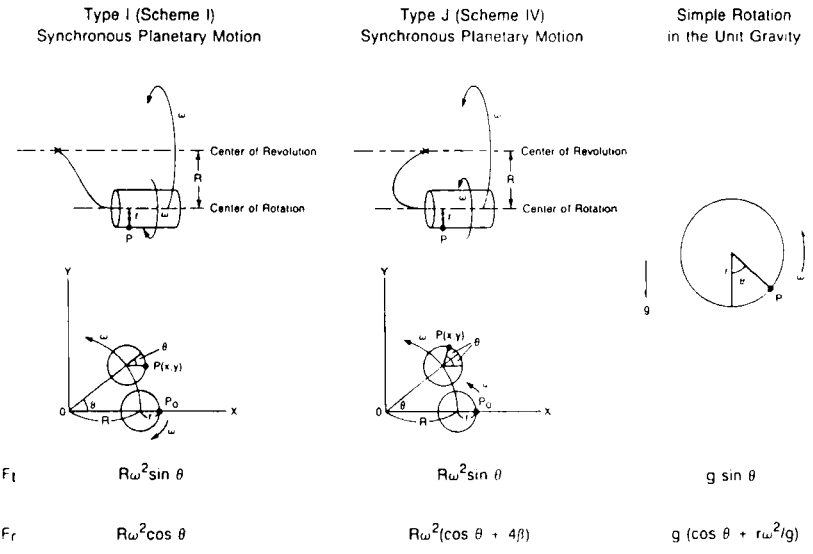

F_t	$R\omega^2 \sin\theta$	$R\omega^2 \sin\theta$	$g \sin\theta$
F_r	$R\omega^2 \cos\theta$	$R\omega^2(\cos\theta + 4\beta)$	$g(\cos\theta + r\omega^2/g)$

FIGURE 6. Comparative studies on three different rotary systems. The tangential (F_t) and the radial (F_r) force components produced by each rotary system are mathematically analyzed. All systems show similar tangential force components while in the radial force components the second term in parentheses, 4β or $r\omega^2/g$, causes asymmetry in the force distribution which in turn produces the unilateral hydrodynamic equilibrium of the two solvent phases in the rotating coil.

systems used for the analysis of the synchronous planetary motion, and the bottom, the mathematical expressions of the two force components, F_t and F_r, acting in each rotary system.

Type I Synchronous Planetary Motion

As shown in Fig. 6 (left), the holder revolves around the central axis of the centrifuge (center of

revolution) at angular velocity ω and synchronously counterrotates about its own axis (center of rotation) located parallel to and at distance R from the center of revolution. Acceleration acting on the holder at arbitrary point P distanced r from the center of rotation can be analyzed by the aid of the coordinate system shown in Fig. 6 (left). The coordinate system is chosen in such a way that the center of revolution is located at the center of the coordinate system while both the center of rotation and the arbitrary point, P_o, are initially present on the x-axis. Then, after time t, the center of rotation circles around point O by $\theta=\omega t$ and the location of the arbitrary point, P (x,y), is expressed by

$$x = R \cos \theta \qquad (1)$$

$$y = R \sin \theta \qquad (2).$$

The acceleration produced by the planetary motion is then obtained from the second derivatives of Eqs. 1 and 2,

$$d^2x/dt^2 = - R\omega^2 \cos \theta \qquad (3)$$

$$d^2y/dt^2 = - R\omega^2 \sin \theta \qquad (4).$$

Since the synchronous counterrotation of the holder maintains the same orientation of point P on the holder, both the radial (F_r) and tangential (F_t) centrifugal force components are directly converted from Eqs. 3 and 4, i.e.,

$$F_r = R\omega^2 \cos \theta \qquad (5)$$

$$F_t = R\omega^2 \sin \theta \qquad (6).$$

Type J Synchronous Planetary Motion

In Type J synchronous planetary motion, the holder revolves around the central axis of the centrifuge at angular velocity ω and synchronously rotates about its own axis in the same direction (Fig. 6, middle). The analysis of acceleration is similarly performed with the coordinate system where the center of the revolution coincides with the center of the coordinate system. For convenience of analysis, the center of the rotation and the arbitrary point are initially located on the x-axis. After the lapse of time t, the holder circles around point O by $\theta=\omega t$ while the arbitrary point circles around the axis of rotation by 2θ. Then, the location of the arbitrary point is found at P (x, y) where

$$x = R \cos \theta + r \cos 2\theta \qquad (7)$$

$$y = R \sin \theta + r \sin 2\theta \qquad (8).$$

The acceleration produced by the planetary motion is then similarly obtained from the second derivatives of Eqs. 7 and 8,

$$d^2x/dt^2 = - R\omega^2(\cos \theta + 4\beta \cos 2\theta) \qquad (9)$$

$$d^2y/dt^2 = - R\omega^2(\sin \theta + 4\beta \sin 2\theta) \qquad (10)$$

where $\beta = r/R$.

The two centrifugal force components, F_r and F_t, are obtained from the above equations according to the following formulae,

$$F_r = -(d^2x/dt^2)\cos 2\theta - (d^2y/dt^2)\sin 2\theta$$
$$= R\omega^2(\cos\theta + 4\beta) \quad (11)$$
$$F_t = -(d^2x/dt^2)\sin 2\theta + (d^2y/dt^2)\cos 2\theta$$
$$= R\omega^2 \sin\theta \quad (12).$$

Simple Rotation in the Unit Gravity

Simple rotation in the unit gravitational field (g) is illustrated in Fig. 6 (right). Point P starts at the bottom and moves in a vertical circle with radius r counterclockwise at angular velocity ω. This motion creates radial centrifugal force field $r\omega^2$. Then, the total force field acting on point P is similarly expressed by two components, F_r and F_t, where

$$F_r = g\cos\theta + r\omega^2 = g(\cos\theta + r\omega^2/g) \quad (13)$$
$$F_t = g\sin\theta \quad (14).$$

Comparative Studies on Three Rotary Systems

The mathematical expressions of F_t and F_r above obtained for each rotary system are indicated in Fig. 6 (bottom) in the respective positions. Comparison between these results first shows that the tangential force components (F_t) in the two types of the synchronous planetary motion are identical, in spite of the fact that these two motions produce contrasting hydrodynamic distribution of the two solvent phases in the coil. Furthermore, this similarity extends to the simple coil

rotation in the unit gravity where the centrifugal term, $r\omega^2$, is simply replaced by the gravitational term, g. This finding strongly suggests that the characteristic hydrodynamic phenomena displayed by these three rotary systems are almost entirely derived from their differences in the radial force components (F_r).

The radial force component (F_r) produced by Type I synchronous planetary motion shows a simple pattern similar to that of the tangential force component (F_t) with a 90 degree shift. The forces acting on the distal and proximal key nodes obtained at $\theta = 0°$ and 180°, respectively, show the equal magnitude both acting in the same direction. On the other hand, the radial force component (F_r) produced by Type J synchronous planetary motion has an additional term, 4ß, in the parentheses that causes asymmetry of the centrifugal force field between the distal and proximal portions of the coil. The force acting at the distal and proximal key nodes are $R\omega^2(4ß \pm 1)$, respectively, and the latter becomes zero at $ß = 0.25$ where the action of the force reverses its direction. At a small ß, the force field approaches that of Type I synchronous planetary motion while the degree of asymmetry becomes greater as ß increases.

The radial force component (F_r) produced by the simple rotation in the unit gravity has a different term relating to the centrifugal force field, $r\omega^2/g$,

indicating that the degree of asymmetry of the force field and the resulting hydrodynamic distribution of the two solvent phases in the coil highly depend upon the rotational speed of the coil. At slow rotation where the centrifugal force is negligible, the radial force field approaches g cos θ (which is comparable to $R\omega^2\cos\theta$ or the radial force component in Type I synchronous planetary motion) and the system similarly establishes the basic hydrodynamic equilibrium of the two solvent phases in the coil. As the rotational speed is increased to generate the centrifugal force, the system gradually develops an asymmetry in the radial force field and at the critical speed range establishes the unilateral hydrodynamic equilibrium where the head phase is determined by the physical properties of the solvent system as described earlier. Because the Archimedean screw force (F_t = g sin θ) produced by the simple rotation never exceeds the unit gravity, the system may also be largely affected by solvent-wall interaction especially at a low rotational speed when a high interfacial tension solvent system is applied to a narrow-bore coil. In this case the solvent phase having the wall-surface affinity could actively creep through the segments of the other phase along the tube wall to occupy the head side of the coil as observed in Type I planetary motion under a low revolution speed [6]. In

the simple rotary system, term $r\omega^2/g$, which causes the asymmetry of the force field, can be further increased by applying a higher rotational speed. Thus the system eventually forms the hydrostatic distribution of the two solvent layers evenly throughout the coil.

In Type J synchronous planetary motion, both tangential and radial force fields linearly increase with the applied centrifugal force field while asymmetry of the force field is produced by term 4ß, which is independent of the revolution speed (ß=r/R). Consequently, the asymmetry of the force field can only be increased by the use of a long rotational radius, r, and/or a short revolution radius, R. However, the maximum ß value available in the standard design of the Type J synchronous coil planet centrifuge is limited to be smaller than 1 and any further increase of ß requires elimination of the central stationary shaft to accommodate the large column holder extending over the central axis of the centrifuge. In the past this type of the coil planet centrifuge had been designed to study the hydrodynamic distribution of two solvent phases in the spiral column with large ß values [7]. The results of the preliminary experiments revealed that an increase of ß range from 0.75-0.95 to 1.5-1.9 produced substantial decrease of the stationary phase retention in all types of the two-phase solvent systems examined. This may

indicate that increase of ß above 1 in Type J synchronous planetary motion tends to shift the phase distribution from the unilateral hydrodynamic equilibrium toward the hydrostatic equilibrium by relatively increasing the radial centrifugal force field as observed in the simple coil rotation in the unit gravity (Fig. 1).

Overall results of the above comparative studies clearly reveal a close relationship between the simple rotation and the two types of the synchronous planetary motion. In the simple rotation under the unit gravity the hydrodynamic distribution takes place in a given magnitude of the Archimedean screw force, $g \sin \theta$, where the superimposed centrifugal force field can sharply increase the asymmetry and the net magnitude of the radial force component. Consequently, the system displays various hydrodynamic distribution patterns ranging from the basic hydrodynamic equilibrium (Stage I) to the unilateral hydrodynamic equilibrium (Stage II and III) and the hydrostatic equilibrium (Stage IV) with further increase of the rotational speed of the coil.

In the synchronous planetary motion where both the tangential force (F_t) and the radial force (F_r) increase linearly with the allied revolution speed, the balance between these two forces can be stably maintained in a broad range of the revolution speed and each type of the synchronous planetary motion establishes a particular

range of the hydrodynamic distribution among the full sequence of hydrodynamic events (Stage I - VI) displayed by the simple coil rotation in the gravity (Fig. 1). In Type I synchronous planetary motion where both F_t and F_r are always comparable to each other in magnitude and symmetry, the system establishes the basic hydrodynamic equilibrium (Stage I) regardless of the helical diameter of the coil. In Type J synchronous planetary motion, where F_r contains an additional term, 4β, to form an asymmetry of the force field, the system displays the unilateral hydrodynamic equilibrium where the head phase being determined by the helical diameter of the coil and the physical properties of the solvent system. For the typical two-phase solvent systems with moderate interfacial tension, heavier phase becomes the head phase in a small helical diameter (Stage II) while in a large helical diameter the lighter phase becomes the head phase (completing the Stage III process).

CONCLUSION

In this paper an attempt has been made to explain various hydrodynamic behaviors of two immiscible solvents observed in the rotating coils. The proposed hypothesis is based on the interplay between two force components: The tangential force component causes the Archimedean screw effect to introduce relative movement of the two

solvent phases along the length of the coil whereas the radial force component interferes with the relative motion of the two solvent phases to establish the hydrostatic equilibrium in the coil. These interactions between the two force components are largely governed by the degree of asymmetry in the radial force field acting on the coil, thus producing various patterns of the hydrodynamic distribution of two solvent phases in the coil.

The hypothesis proposed in this paper successfully rationalizes all the hydrodynamic phenomena in the rotating coils reported in the past. However, the present hypothesis may be one of many that can equally well explain the observed hydrodynamic phenomena and final justification of the hypothesis remains open to future investigation.

REFERENCES

1. Ito, Y., Countercurrent chromatography (miireview), J. Biochem. Biophys. Methods, 5, 105, 1981.

2. Ito, Y., Development of high-speed countercurrent chromatography, Advances in Chromatography, Marcel Dekker, New York vol 24, edited by J. C. Giddings, E. Grushka, J. Cazes and P.R. Brown, Chapter 6, 1984, p.181.

3. Ito, Y. and Bhatnagar, R., Preparative countercurrent chromatography with a rotating coil assembly, J. Chromatogr., 207, 171, 1981.

4. Ito, Y., A new horizontal flow-through coil planet centrifuge for countercurrent chromatography: II. The apparatus and its partition capabilities, J. Chromatogr., 188, 43, 1980.

5. Ito, Y., Experimental observations of the hydrodynamic behavior of solvent systems in high-speed countercurrent chromatography: Part I. Hydrodynamic distribution of two solvent phases in a helical column subjected to two types of synchronous planetary motion, J. Chromatogr., 301, 377, 1984.

6. Ito, Y. and Bowman, R.L., Countercurrent chromatography with the flow-through coil planet centrifuge, J. Chromatogr. Sci., 11, 284, 1973.

7. Ito, Y., Experimental observations of the hydrodynamic behavior of solvent systems in high-speed countercurrent chromatography: Part II. Phase distribution diagrams for helical and spiral columns, J. Chromatogr., 301, 387, 1984.

8. Ito, Y. and Conway, W.D., Experimental observation of the hydrodynamic behavior of solvent systems in high-speed countercurrent chromatography: Part III. Effects of physical properties of the solvent systems and operating temperature on the distribution of two-phase solvent systems, J. Chromatogr., 301, 405, 1984.

9. Conway, W.D. and Ito, Y., Phase distribution of liquid-liquid systems in spiral and multi-layer helical coils in a centrifugal countercurrent chromatography, presented at the 1984 Pittsburgh Conference and Exposition on Analytical Chemistry and Applied Spectroscopy, No.472.

10. Sutherland, I.A. and Heywood-Waddington, D., Hydrodynamic of liquid-liquid system in a spiral section of multilayer coil planet centrifuge, presented at the 1985 Pittsburgh Conference and Exposition on Analytical Chemistry and Applied Spectroscopy, No.302.

11. This manuscript was prepared in 1986 and since then it has been kept in the author's drawer without publication. Although a number of papers have been published on countercurrent chromatography during the past 6 years, the present hypothesis is still standing without any serious discrepancy against the experimental findings.